SANDIA REPORT

SAND2017-12409
Unlimited Release
Printed November 2017

SNL/JAEA Collaboration on Sodium Fire Benchmarking

Andrew J. Clark, Matthew R. Denman, Takashi Takata, Hiroyuki Ohshima

Prepared by
Sandia National Laboratories
Albuquerque, New Mexico 87185 and Livermore, California 94550

Sandia National Laboratories is a multimission laboratory managed and operated by National Technology and Engineering Solutions of Sandia, LLC, a wholly owned subsidiary of Honeywell International, Inc., for the U.S. Department of Energy's National Nuclear Security Administration under contract DE-NA0003525.

Issued by Sandia National Laboratories, operated for the United States Department of Energy by National Technology and Engineering Solutions of Sandia, LLC.

Available to DOE and DOE contractors from
U.S. Department of Energy
Office of Scientific and Technical Information
P.O. Box 62
Oak Ridge, TN 37831

Telephone: (865) 576-8401
Facsimile: (865) 576-5728
E-Mail: reports@osti.gov
Online ordering: http://www.osti.gov/scitech

Available to the public from
U.S. Department of Commerce
National Technical Information Service
5301 Shawnee Rd
Alexandria, VA 22312

Telephone: (800) 553-6847
Facsimile: (703) 605-6900
E-Mail: orders@ntis.gov
Online order: http://www.ntis.gov/search

SAND2017-12409
Printed November 2017
Unlimited Release

SNL/JAEA Collaboration on Sodium Fire Benchmarking

Andrew J. Clark and Matthew R. Denman
Risk and Reliability Analysis
Sandia National Laboratories
P. O. Box 5800
Albuquerque, New Mexico 87185-MS0748

Takashi Takata and Hiroyuki Ohshima
Fast Reactor Computational Engineering Department
Advanced Fast Reactor Cycle System Research and Development Center
Japan Atomic Energy Agency
Oarai, Japan

Abstract

Two sodium spray fire experiments performed by Sandia National Laboratories (SNL) were used for a code-to-code comparison between CONTAIN-LMR and SPHINCS. Both computer codes are used for modeling sodium accidents in sodium fast reactors. The comparison between the two codes provides insights into the ability of both codes to model sodium spray fires. The SNL T3 and T4 experiments are 20 kg sodium spray fires with sodium spray temperatures of 200°C and 500°C, respectively. Given the relatively low sodium temperature in the SNL T3 experiment, the sodium spray experienced a period of non-combustion. The vessel in the SNL T4 experiment experienced a rapid pressurization that caused of the instrumentation ports to fail during the sodium spray. Despite these unforeseen difficulties, both codes were shown in good agreement with the experiments. The subsequent pool fire that develops from the unburned sodium spray is a significant characteristic of the T3 experiment. SPHINCS showed better long-term agreement with the SNL T3 experiment than CONTAIN-LMR. The unexpected port failure during the SNL T4 experiment presented modelling challenges. The time at which the port failure occurred is unknown, but is believed to have occurred at about 11 seconds into the sodium spray fire. The sensitivity analysis for the SNL T4 experiment shows that with a port failure, the sodium spray fire can still maintain elevated pressures during the spray.

ACKNOWLEDGMENTS

The authors would like to thank Sandia staff members Fred Gelbard, David Louie, and Vincent Mousseau for providing a technical review of this document. The authors would also like to thank JAEA staff members Toru Makino and Yuji Tajima for their technical support of computations.

TABLE OF CONTENTS

LIST OF FIGURES

LIST OF TABLES

NOMENCLATURE

CNWG	Civil Nuclear Energy Research and Development Working Group
JAEA	Japan Atomic Energy Agency
Na	Sodium
Na_2O	Sodium Monoxide
Na_2O_2	Sodium Peroxide
O_2	Oxygen Gas
SFR	Sodium Fast Reactor
SNL	Sandia National Laboratories
SPHINCS	Sodium Fire Phenomenology in Multi-Cell System

1. INTRODUCTION

The energetic combustion of sodium with oxygen resulting from sodium leaks is a critical issue to the plant safety for sodium-cooled fast reactors (SFRs). Sodium leaks, typically from the primary or secondary SFR coolant loops, can result in sodium spray fires when sodium reacts with oxygen or water vapor in the air. High-temperature (usually defined to be greater than 200°C) sodium sprays readily react with oxygen and water vapor in the air, which results in strongly exothermic reactions. The smaller the spray droplets for the same amount of sodium, the more severe the containment or cell response will be due to a larger surface-to-volume ratio. For coarse droplets, some of the sodium sprayed will not react, leading to a subsequent pool fire.

Sodium leaks and subsequent sodium fire events have been recorded at various SFRs around the world. One such event occurred at the Monju prototype fast breeder reactor when sodium leaked from the secondary coolant loop and a subsequent fire took place [1]. Due to the occurrence and potential severity of sodium leak events, computer codes have been developed to evaluate containment responses and potential source term releases. CONTAIN-LMR and SPHINCS are two such numerical tools that incorporate mechanistic models for sodium combustion.

CONTAIN is a best-estimate, integrated analysis tool for predicting the physical, chemical, and radiological conditions inside a nuclear reactor containment building following the release of core or coolant material from the primary system [2]. CONTAIN-LMR is a code version of CONTAIN that allows for the analysis of sodium coolant [3]. CONTAIN and CONTAIN-LMR were developed by Sandia National Laboratories (SNL). The sodium chemistry models developed for CONTAIN-LMR are currently being integrated into the MELCOR computer code at SNL for the U.S. Nuclear Regulatory Commission [4, 5]. SPHINCS, which stands for Sodium fire PHenomenology IN multi-Cell System, is a fast-running, zone model and sodium combustion computer code extensively used for sodium safety evaluation that was developed by Japan Atomic Energy Agency (JAEA) [6].

Recently, SNL and JAEA have exchanged information of sodium combustion modelling and related experimental data. This is being done collaboratively in the field of advanced reactor modelling and simulation in Civil Nuclear Energy Research and Development Working Group (CNWG). The first phase of this collaboration includes a code-to-code benchmark analysis of the SNL Surtsey spray fire experiments using CONTAIN-LMR (SNL) and SPHINCS (JAEA). The second phase of this collaboration will analyse sodium pool fire experiments, and will be described in future reports.

The next subsection provides an introduction of the spray fire experiments performed at SNL. Section 2 of this report will describe the mechanistic models that are employed in both the CONTAIN-LMR and SPHINCS computer codes. Section 3 presents best-estimate results and sensitivity analysis of the SNL T3 experiments using CONTAIN-LMR and SPHINCS. Similarly Section 4 presents best-estimate results and sensitivity analysis of the SNL T4 experiment. Section 5 summarizes the analyses performed.

1.1. Sodium Spray Fire Experiments at SNL

In 2008 and 2009, SNL performed a series of sodium pool and spray fire experiments [7]. Four spray fire experiments were performed: two outdoor experiments (T1 and T2) and two indoor experiments (T3 and T4). The outdoor experiments were initial scoping experiments.

The SNL sodium spray fire experiments T3 and T4 were carried out in the Surtsey vessel located at SNL in Albuquerque, NM. Several measurements were taken during these experiments including: vessel pressure, thermocouple measurements in air and on vessel walls, total radiative heat flux, and videography of the experiments inside the vessel. Vessel pressure and thermocouple measurements are used for comparing experiments with the computer code simulations. The videography has been investigated to explain phenomena related to the experimental data results.

The Surtsey vessel, shown in Figure 1-1, has a cylindrical shape and is 3.6 m in diameter and 10.3 m high, with a total volume of about 100 m^3. The vessel contains various ports that allow for instrumentation and piping to be fed into the vessel. Prior to the spray, sodium was heated inside a heater tank located outside of the vessel. The Surtsey vessel was at atmospheric pressure while the sodium heater tank was pressurized to 307 psig (2,117 kPa) and heated to the desired temperature for each experiment. The piping for sodium injection led from the heater tank outside the vessel to inside the vessel. The H15 type nozzle used to create the spray was located 5.3 m above the floor of the vessel. In both experiments, about 20 kg of sodium was injected into the vessel at an estimated flowrate for 1 kg/s. The primary difference between experiment T3 and T4 is the sodium temperature, which was 200°C for T3 and 500°C for T4, which is above the sodium melting point.

Figure 1-1. SNL Surtsey vessel located in Albuquerque, NM.

2. MODELING OF SODIUM SPRAY FIRES

The following section describes the models used to predict the spray burn rate and energy released from sodium spray fires. The sodium spray fire models of CONTAIN-LMR and SPHINCS are based on the NACOM code [8]. A summary of the spray fire mode from the NACOM code is provided, followed by a discussion on the NACOM model implemented to CONTAIN-LMR and SPHINCS.

Sodium spray fire combustion is modeled using single droplet vapor phase combustion theory, which is well established for combustion of hydrocarbon fuel droplets. The NACOM code models reactions of sodium with water vapor and oxygen in the air. CONTAIN-LMR and SPHINCS have been simplified to only model reactions of sodium and oxygen. Two reactions may occur to form either sodium monoxide (Na_2O) or sodium peroxide (Na_2O_2). The reactions, along with the corresponding combustion energy, are provided in Equations (2-1) and (2-2) below [8].

$$2Na + \tfrac{1}{2}O_2 \rightarrow Na_2O \quad \Delta H_{rxn} = 9.18\times10^6\ J \tag{2-1}$$

$$2Na + O_2 \rightarrow Na_2O_2 \quad \Delta H_{rxn} = 10.46\times10^6\ J \tag{2-2}$$

Sodium monoxide melts at 1,132°C and decomposes at 1,950°C. Sodium peroxide melts at 674°C and decomposes at 1,627°C [8].

Figure 2-1 provides an overview of the models in the SPHINCS and CONTAIN-LMR codes. One model option that is not shown in Figure 2-1 is the atmospheric chemistry models. The atmospheric chemistry model provides additional sources of energy due to chemical reactions in the aerosol phase.

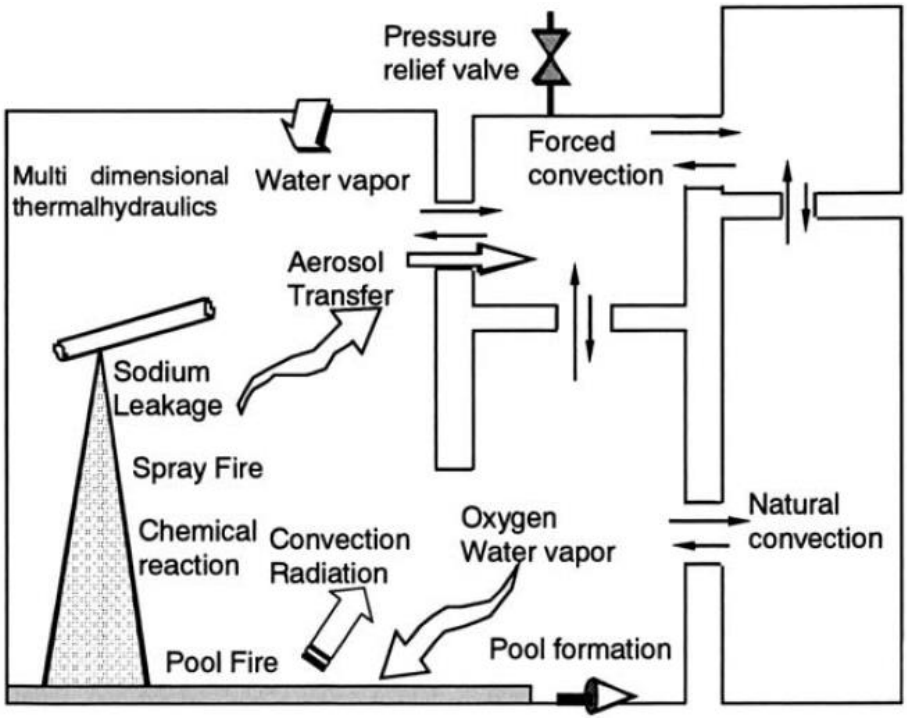

Figure 2-1. Models used in the SPHINCS and CONTAIN-LMR computer codes [6]. The partitions represent the separation of cells that can be used to model the transport of fluids between cells.

Several phenomena that effect sodium spray combustion are not modeled in CONTAIN-LMR or SPHINCS. The first phenomena is the local oxygen concentration in the spray zone. Sodium combustion within the cone of the spray will deplete the oxygen in the spray zone, especially for high temperature sodium. Assuming that all the oxygen in the vessel is available for combustion can lead to overestimation of the total sodium combustion. The second phenomena that is not modeled is the interaction of falling droplets. There are statistical challenges to modeling interaction of falling droplets and rather than attempt to model this complex phenomena, the interaction has been neglected for the current models. Assuming that droplets could interact and coagulate, this would lead to less surface area for the same amount of sodium which would result in an overall decrease of sodium combustion. Neglecting both of these phenomena from the models results in conservative predictions of the total sodium combustion and the total energy released.

2.1. Sodium Droplet Burning Rate for Falling Droplets

The vapor phase combustion theory employed by NACOM is for a single, stationary, spherical, burning droplet. For the stationary droplet assumption, the flame zone (burning zone) is assumed to be symmetrical around the droplet, as shown in Figure 2-2. The droplet burning rate is controlled by the evaporation of sodium from the surface to the flame zone. Evaporation is controlled by the rate of heat transfer to the droplet.

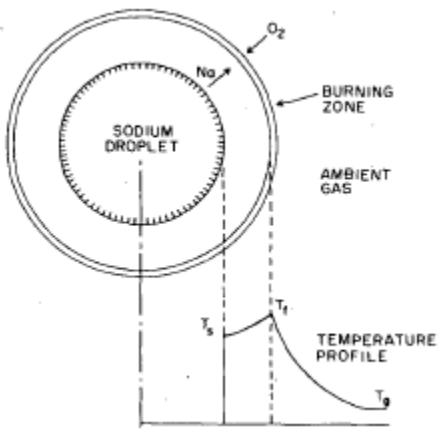

Figure 2-2. Schematic of a stationary, spherical burning droplet [8].

Burning of a spherical, stationary droplet follows the "D^2" law, which is given in Equation (2-3).

$$\frac{d(D^2)}{dt} = -\frac{4\dot{m}}{\pi\rho D} \tag{2-3}$$

In the above equation, D is the droplet diameter, t is time, $\dot{m}$ is the mass burning rate for a spherical, stationary sodium droplet, and ρ is the sodium droplet density. The negative of the left-hand side of Equation (2-3) is termed the evaporation rate constant, K. Equation (2-3) may be rearranged to express the mass burning rate as a function of the evaporation constant and droplet diameter.

$$\dot{m} = \frac{\pi\rho K}{4} D \tag{2-4}$$

As the droplet burns, the diameter of the droplet will decrease over time. The linear relationship between D^2 and t is given in Equation (2-5).

$$D^2 = D_i^2 - Kt \tag{2-5}$$

In Equation (2-5), D_i represents the initial droplet diameter. The evaporation rate constant K can be calculated using the Spalding number B.

$$K = \frac{8k}{C_p \rho} \ln(1 + B) \tag{2-6}$$

$$B = \frac{1}{h_{fg}} \left[C_P (T_g - T_s) + \frac{H_c Y}{i} \right] \tag{2-7}$$

In the two equations above, k is the thermal conductivity of the gas, C_p is the heat capacity of the gas, h_{fg} is the heat of evaporation, T_g is the average gas temperature, T_s is the sodium droplet temperature, H_c is the heat of combustion, Y is the ambient oxygen mole fraction, and i is the stoichiometric ratio (the mass ratio of reacting oxidizer to sodium).

As noted, Equation (2-4) applies to a stationary, spherical burning droplet, but as a droplet falls towards the ground, forced convection across the droplet causes the flame zone around the droplet to become distorted. As reported in [9], multiple investigators treat forced convection by employing a multiplication factor to the stationary, spherical burning droplet equation. The mass burning rate for forced convection, $\dot{m}_f$, is given by Equation (2-8) below.

$$\dot{m}_f = \dot{m}(1 + C_f Re^{1/2} Pr^{1/3}) \tag{2-8}$$

The two non-dimensional number in Equation (2-8) are the Reynolds number, Re, and the Prandtl number, Pr. The empirical constant C_f in Equation (2-8) is assigned a value of 0.3 in the NACOM code as this value correlated well with the results provided in [9].

Sodium combustion can be divided into a pre- and post-ignition phase. Prior to ignition, the amount of evaporation is relatively small, but a coarse oxide film is formed on the droplet. The oxide film causes a large portion of the combustion heat from Equations (2-1) and (2-2) to be redirected to the sodium droplet causing the droplet temperature to increase.

NACOM uses a surface oxidation model for the pre-ignition phase, which was first proposed by Tsai [9]. The Ranz-Marshall correlation [10] is used to predict oxygen diffusion to the droplet surface. The sodium droplet burning rate during pre-ignition is obtained from the oxygen flux and the stoichiometric ratio.

$$\dot{m}_f = \frac{\pi C D_d Y D}{i} (2 + 0.6 Re^{1/2} Sc^{1/3}) \tag{2-9}$$

In Equation (2-9), C and D_d represent the mass concentration of oxygen and its diffusivity in air, respectively. The Prandtl number Pr is replaced in Equation (2-9) with the Schmidt number, Sc, to reflect the Ranz-Marshall correlation for the oxygen flux.

Post-ignition burning for falling droplets is given in Equation (2-10).

$$\dot{m}_f = 2\pi \frac{kD}{C_p} \ln(1+B)(1+0.3Re^{1/2}Pr^{1/3}) \tag{2-10}$$

2.2. Sodium Droplet Size Distribution

Spray dynamics use liquid droplet size bins to determine the number of liquid droplets with different diameters. For both CONTAIN-LMR and SPHINCS, the Nukiyama-Tanasawa distribution is used to represent the statistical characteristics of the liquid drop size [8]. The volume fraction F that the droplet diameter is equal to or smaller than D is given by Equation (2-11).

$$\frac{dF}{dD} = \left(\frac{3.915}{\overline{D}}\right)^6 \frac{D^5}{120} \exp\left(-\frac{3.915D}{\overline{D}}\right) \tag{2-11}$$

$\overline{D}$ in Equation (2-11) is the volume-average diameter. Because the interaction of droplets is ignored, the volume fraction determined by Equation (2-11) does not change during the droplet fall. However, the volume-average diameter in a given population will change as combustion occurs. The Lagrangian method is used to track the burning of droplets from origination to the floor.

2.3. Sodium Spray Fire Modeling in CONTAIN-LMR

The NACOM models used for modeling sodium spray fires have been adopted into CONTAIN-LMR, with some key differences. In NACOM, the velocity of the droplets is calculated from Newton's law of motion and also accounts for the effects of vaporization on the drag force. CONTAIN-LMR, on the other hand, calculates the terminal velocity of the droplets, and that velocity is the velocity of the droplets from origination to the floor.

Another modification is that the combustion energy is computed based on the mole fraction of sodium to peroxide ($F_{peroxide}$), which is given by Equation (2-12) [5].

$$S = \frac{1.3478 \cdot F_{peroxide}}{1.6957 - 0.3479 \cdot F_{peroxide}} \tag{2-12}$$

Heat of combustion, E_{spray} (J), is then calculated according to Equation (2-13) [5].

$$E_{spray} = (1-S) \cdot 9.18 \times 10^6 + S \cdot 10.46 \times 10^6 \tag{2-13}$$

CONTAIN-LMR [3] is a keyword driven code that requires the sodium spray fire models to be called by the user in the input deck. The spray fire model, SPRAFIRE, in CONTAIN-LMR requires four user inputs: fall height of sodium spray [HITE], mean sodium droplet diameter [DME], mole fraction of sodium peroxide produced by the fire [FNA2O2], and the source injection rate of sodium [SOURCE]. The source requires several other inputs, including the spray duration, mass flow rate of sodium, and either the temperature or enthalpy of the sodium source.

While the current analysis described in this report uses the CONTAIN-LMR computer code, [5] describes the ongoing efforts at SNL to transfer the CONTAIN-LMR models into MELCOR.

2.4. Sodium Pool Fire Modeling

Any sodium that does not combust before hitting the floor will be added to the sodium pool. After all the sodium has sprayed, the non-combusted sodium effects the long-term vessel response and needs to be accounted for as will be shown in the sensitivity analysis. A high level summary of the CONTAIN-LMR and SPHINCS models is provided here, but the technical details of the pool fire models are planned to be described in future reports.

The sodium pool fire models used in CONTAIN-LMR are adopted from SOFIRE II [11] and are documented in [5]. Similar to the spray fire model, the pool fire model must be identified by the user in the input deck, otherwise the pool fire models will not be employed in the simulation. There are four parameters that must be allocated by the user when modeling the sodium pool fire, which are the following:

- *f1* is the fraction of total oxygen consumed that reacts to form sodium monoxide, where the balance (1−*f1*) reacts to form sodium peroxide,
- *f2* is the fraction of sensible heat that is transferred to the pool, where the balance (1−*f2*) is transferred to the atmosphere,
- *f3* is the fraction of Na_2O product that enters the pool as a solid after formation, where the balance (1−*f3*) enters the atmosphere as an aerosol, and
- *f4* is the fraction of Na_2O_2 product that enters the pool as a solid after formation, where the balance (1−*f4*) enters the atmosphere as an aerosol.

The main pool fire reaction for the sodium pool fire model is given in Equation (2-14) [5].

$$(1+\mathrm{f1})\cdot 2\cdot \mathrm{Na}+\mathrm{O_2}\rightarrow 2\cdot \mathrm{f1}\cdot \mathrm{Na_2O}+(1-\mathrm{f1})\cdot \mathrm{Na_2O_2}+\mathrm{Q_{rxn}} \tag{2-14}$$

Q_{rxn} in Equation (2-14) is also a function of *f1* and represents the heat of reaction added to the system based Equations (2-1) and (2-2). Equation (2-14) requires oxygen in the air to diffuse to the sodium pool. The diffusion constant for oxygen-nitrogen mixtures used in CONTAIN-LMR differs from that used in SOFIRE-II. The diffusion constant, $D_O\,(\mathrm{m^2/s})$, used in CONTAIN-LMR is described in [12] and is shown in Equation (2-15).

$$\mathrm{D_O}=6.4315\times 10^{-5}\,\frac{\mathrm{T_{film}^{1.823}}}{\mathrm{P}} \tag{2-15}$$

In Equation (2-15), T_{film} is the average pool temperature (K) and *P* the system pressure (Pa). For further details on the heat transfer and heat flux to/from the pool, the reader is referred to [5] and [12].

The details of the sodium ring pool fire model developed for the SPHINCS code are provided in [6] and a summary of the model is presented here. The ring pool fire model is a flame sheet model that is divided into a number of concentric rings with the flame sheet model applied to each ring. The flame sheet model calculates the molar flux of sodium from the surface of the pool the flame sheet and the molar flux of oxidizer from the atmosphere to the flame sheet. Flame height and flame temperature are determined from mass and energy balances at the flame zone. Heat transfer from the flame to the atmosphere occurs by convection and radiation and from the flame to the pool it occurs by conduction and radiation.

2.5. Summary

The sodium spray fire model in both CONTAIN-LMR and SPHINCS is obtained from the NACOM code. The most significant difference that results from the implementation of the NACOM code into CONTAIN-LMR and SPHINCS is the determination of the droplet velocities by both codes. Where CONTAIN-LMR uses the terminal velocity, SPHINCS calculates the fall velocity for each droplet size bin as a function of time using Newton's equations of motion.

In the following sections, the ability of each code to predict two of SNL's sodium spray fire experiments is demonstrated. Sensitivity analysis are also performed to investigate the effects that specific parameters have on the overall predictions.

3. SNL T3 SODIUM SPRAY FIRE MODELING RESULTS

Key input parameters for CONTAIN-LMR and SPHINCS are provided in Table 3-1, which represent the initial conditions of the T3 experiment as closely as possible. As noted in Section 2.4, the sodium pool fire formed from unburned sodium during the spray has a substantial effect on the long-term pressure and temperature responses. Since the primary focus of this report is on the spray fire modeling, the default parameters for the sodium pool fire model are used for the T3 simulation. Also, the atmospheric chemistry model is activated.

Table 3-1. Summary of key input parameters for SNL T3 experiment.

Parameter	CONTAIN-LMR	SPHINCS
Vessel free volume	99 m^3	99 m^3
Vessel thickness	0.11 m	0.11 m
Vessel wall emissivity	0.9 [-]	0.9 [-]
Nozzle height	5.3 m	5.3 m
Sodium outlet nozzle velocity	Terminal Velocity	9.34 m/s
Initial sodium temperature	200°C	200°C
Mean droplet diameter (volumetric mean)	2.45 mm	2.75 mm
Sodium pool fire model	Activated	Activated
Atmospheric chemistry model	Activated	Activated
Initial gas temperature	15°C	15°C
Initial gas pressure	101.3 kPa	101.3 kPa
Oxygen concentration (molar fraction)	0.21 [-]	0.21 [-]
Pool fire parameters (*f1, f2, f3, f4*)	0.5, 1.0, 1.0, 0.0	Ring Pool Fire Model [6]

The sodium droplet diameter reported in [7] was 3-5 mm. The basis for this droplet diameter is uncertain. Based on the uncertain diameters reported, the approach taken in this analysis was to use the experimental initial conditions and then fit the computer code results to the experimental peak pressure by varying the mean droplet diameter. This resulted in a diameter of 2.45 mm for CONTAIN-LMR and 2.75 mm for SPHINCS.

In addition to the parameters listed in Table 3-1, the user-defined fraction of peroxide formed during spray combustion was set to 1.0 as a first approximation. According to [5], this value seems to agree well with experimental data from sodium sprays. Analysis of the chemical composition of the products produced from the spray and subsequent pool were not recorded in SNL T3 and T4 experiments.

The CONTAIN-LMR and SPHINCS best-estimate results for pressure and temperature responses are shown in Figure 3-1 and Figure 3-2, respectively. In each figure, short term responses (0-100 seconds) are shown on the left and long term responses (0-1,000 seconds) are shown on the right.

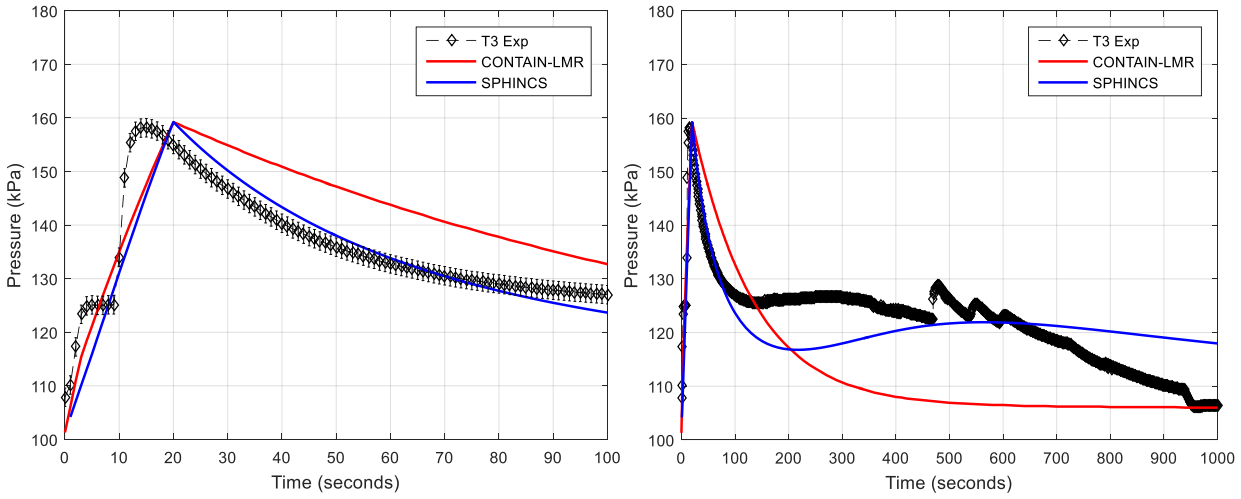

Figure 3-1. T3 pressure responses for best-estimate inputs for CONTAIN-LMR (red line) and SPHINCS (blue line) compared to T3 experimental data. Short term responses are shown on the left and long term responses are shown on the right.

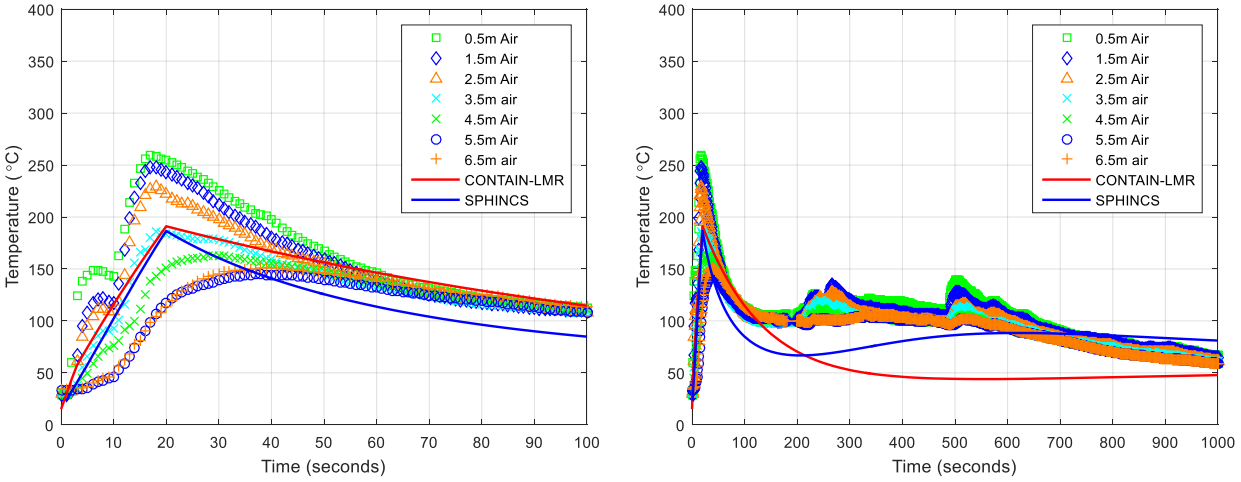

Figure 3-2. T3 temperature responses for best-estimate inputs for CONTAIN-LMR (red line) and SPHINCS (blue line) compared to T3 experimental data. Short term responses are shown on the left and long term responses are shown on the right.

The short term responses in the left plots of Figure 3-1 and Figure 3-2 agree quite well with experimental data during the spray. CONTAIN-LMR and SPHINCS have similar pressure and temperature rises during the duration of the spray, with the difference likely influenced by how the two codes determine velocity of droplets (see Section 2.3). After the spray is completed (from 20-100 seconds), the short term (left plots) vessel pressure response is better predicted by SPHINCS, whereas the temperature response is better predicted by CONTAIN-LMR.

The long term responses in the right plots of Figure 3-1 and Figure 3-2 have noticeable discrepancies compared to the experimental data. The most likely reason for the discrepancies is due to multiple small pools being formed on the floor of the vessel, rather than one large pool modeled by CONTAIN-LMR and SPHINCS. Compared to one large pool, multiple small pools would increase the surface-to-volume ratio leading to increased combustion energy produced. At about 250 seconds, there is both a pressure and temperature increase. This phenomenon is likely

attributed to the pool temperatures increasing to a point where combustion is significantly increased; the pool temperature increase is due to the reaction energy released from pool combustion. The lower thermocouple measurements (namely 0.5m Air to 3.5m Air) in the right plot of Figure 3-2 experience the largest increase at this time, which may support this speculation. SPHINCS also captures this phenomenon, but at a later time than what is observed from the experimental data. CONTAIN-LMR does not capture this phenomenon, but *f2* can possibly be varied to better model this phenomenon. The total sodium burned during the spray and pool fires are listed in Table 3-2 for each of CONTAIN-LMR and SPHINCS.

Table 3-2. Total sodium burned during SNL T3 spray and pool fires for CONTAIN-LMR and SPHINCS.

	CONTAIN-LMR	SPHINCS
Sodium Spray Fire	4.26 kg	3.85 kg
Sodium Pool Fire	1.27 kg	16.15 kg

In addition to CONTAIN-LMR and SPHINCS responses, several features should be highlighted with respect to the experimental data. First, between three and nine seconds, the pressure response (and several thermocouple measurements) plateaus, which seems to indicate that no combustion is occurring. This hypothesis is further supported by investigation of the T3 videography.

Second, the experimental peak pressure occurs at about 14 seconds, whereas the computer code results have a peak pressure at 20 seconds. The 1 kg/s reported in [7] was an estimate not supported by any flow rate measurements. Based on the experimental results, it is more likely that the spray duration was 14 seconds, resulting in a flowrate of 1.43 kg/s. This flowrate is explored in the following T3 sensitivity analysis section.

Third, the experimental data starts to fluctuate at about 490 seconds which is most likely due to the experimenters starting to vent the Surtsey vessel. The opening of the vents would replenish some of the reacted oxygen leading to enhanced combustion, which explains the pressure rise at about 500 seconds. However, the exact timing at which the experimenters opened the vents was not recorded, but is said to have occurred sometime after 10 minutes (300 seconds).

3.1. SNL T3 Sodium Spray Fire Sensitivity Analysis

The following sections highlight sensitivity of the spray fire models as well as sensitivities addressing experimental uncertainties for the SNL T3 experiment. The sensitivity analysis only compares pressure responses because including the temperature responses would result in numerous lines on a single plot which reduces the ability to interpret the results meaningfully.

3.1.1. Sodium Mean Droplet Diameter Sensitivity

The most sensitive parameter for sodium spray fire analysis is the sodium mean droplet diameter. This is mainly due to the "D^2" law highlighted by Equation (2-5). For the sensitivity analysis, the mean droplet diameter was set to 2.0 mm and 3.0 mm for both codes. This sensitivity analysis is provided in Figure 3-3.

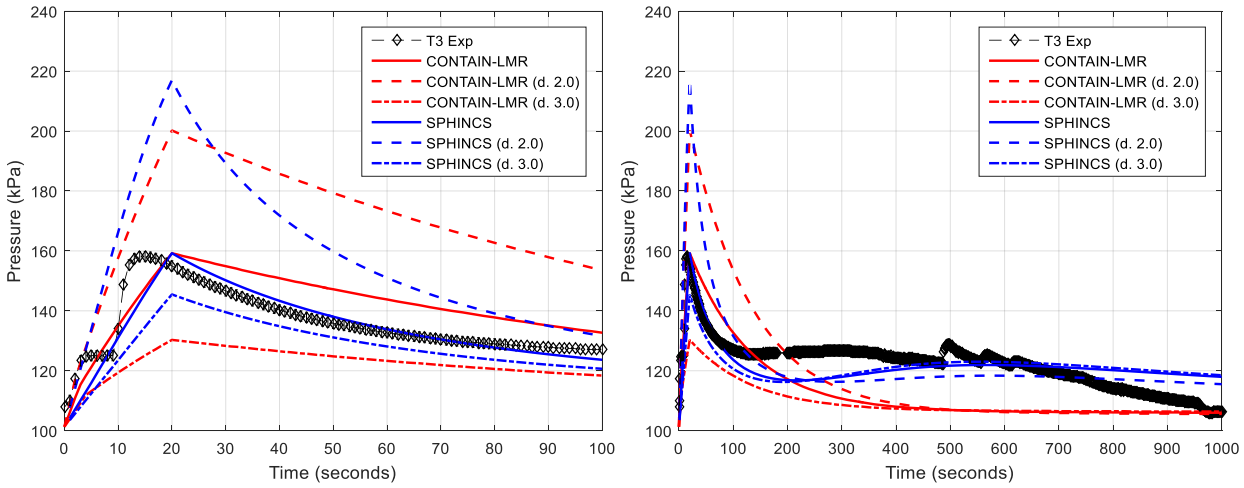

Figure 3-3. T3 pressure responses for mean droplet diameter sensitivity analysis for CONTAIN-LMR (red lines) and SPHINCS (blue lines). Short term responses are shown on the left and long term responses are shown on the right.

Figure 3-3 demonstrates the "D^2" law where a small decrease in the mean droplet diameter results in a large peak pressure increase. For a mean droplet diameter of 2.0 mm, the peak pressure increase for CONTAIN-LMR was about 25% greater than the best-estimate case (2.45 mm) and about 36% greater than the best-estimate case (2.75 mm) for SPHINCS. For a mean droplet diameter of 3.0 mm, both codes resulted in a decrease of the overall peak pressure. The total sodium combusted during the spray for each mean droplet diameter is provided in Table 3-3.

Table 3-3. Total amount of sodium combustion during T3 spray for each mean droplet diameter input.

Mean Droplet Diameter	CONTAIN-LMR	SPHINCS
Best Estimate (see Table 3-1)	4.26 kg	3.85 kg
2.0 mm	6.03 kg	7.45 kg
3.0 mm	2.92 kg	3.04 kg

The effect on the long term pressure response (right plot in Figure 3-3) was not as pronounced as for the short term response. CONTAIN-LMR results all reach a steady pressure at about 420 seconds regardless of the droplet diameter. SPHINCS long term results for a diameter of 3.0 mm closely align with the best-estimate case. When the mean droplet diameter is 2.0 mm, the secondary pressure increase is not as significant. This is likely due to more sodium combusting during the spray which reduces the overall sodium available for pool combustion.

3.1.2. Sodium Spray Duration Sensitivity

It was noted in the Section 3 that the time at which the experimental peak pressure occurred supports a 14 second spray duration, instead of a 20 second spray duration as reported in [7]. By assuming a 14 second spray that injects 20 kg of sodium, the mass flowrate is 1.43 kg/s. The results of this analysis are plotted in Figure 3-4 with all other parameters as reported in Table 3-1.

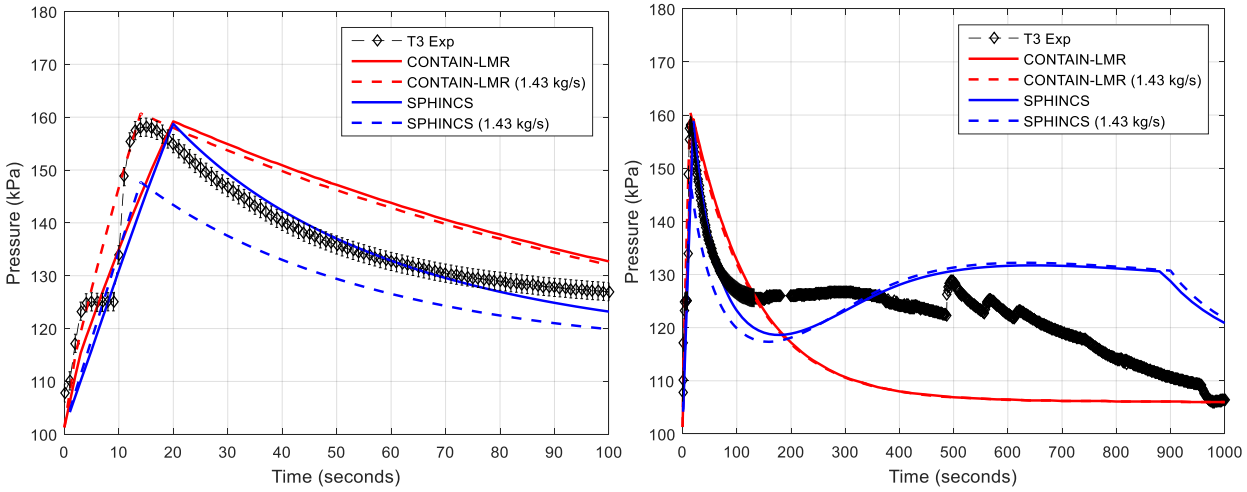

Figure 3-4. T3 pressure responses for mass flow rate sensitivity analysis for CONTAIN-LMR (red lines) and SPHINCS (blue line). Short term responses are shown on the left and long term responses are shown on the right.

For CONTAIN-LMR, the increased mass flowrate results in a slightly higher peak pressure than the experimental peak pressure, but the peak pressure occurs at the same time as the experimental peak pressure. For SPHINCS, the peak pressure for a 14 second spray duration results in a peak pressure that is less than the experimental peak pressure. For the same mean droplet diameter, the increased mass flowrate results in slightly more sodium combustion for CONTAIN-LMR and less sodium combustion for SPHINCS, as shown in Table 3-4. For SPHINCS, the increased mass flow rate leads to an increased outlet spray velocity which results in a reduction of the peak pressure and amount of sodium combustion. In the absence of mass flowrate measurements, the authors believe that a 14 second spray was the true spray duration for both the T3 and T4 experiments. For the rest of the T3 and T4 analysis, the 14 second spray duration is applied.

Table 3-4. Total amount of sodium combustion during T3 spray for 20 second (best estimate) and 14 second spray durations.

Spray Duration	CONTAIN-LMR	SPHINCS
Best Estimate (see Table 3-1)	4.26 kg	3.85 kg
14 Seconds	4.27 kg	3.19 kg

3.1.3. CONTAIN-LMR Pool Fire Parameter f2 Sensitivity

The default pool fire parameter *f2* is 1.0, as listed in Table 3-1. With an *f2* parameter value of 1.0, only a small amount of energy is being transferred from the pool to the surroundings; only radiative heat transfer is occurring from the pool to the surroundings. Decreasing the *f2* parameter will cause more heat of reaction to be transferred to the atmosphere versus the pool (see Section 2.4). Consequently, as *f2* decreases, less reaction heat is transferred to the pool which results in an overall decrease of sodium pool combustion. The pool fire parameter *f2* sensitivity was explored with values of 0.9, 0.5, and 0.1, as shown in Figure 3-5. The overall sodium combustion for each of the listed parameter values is presented in Table 3-5.

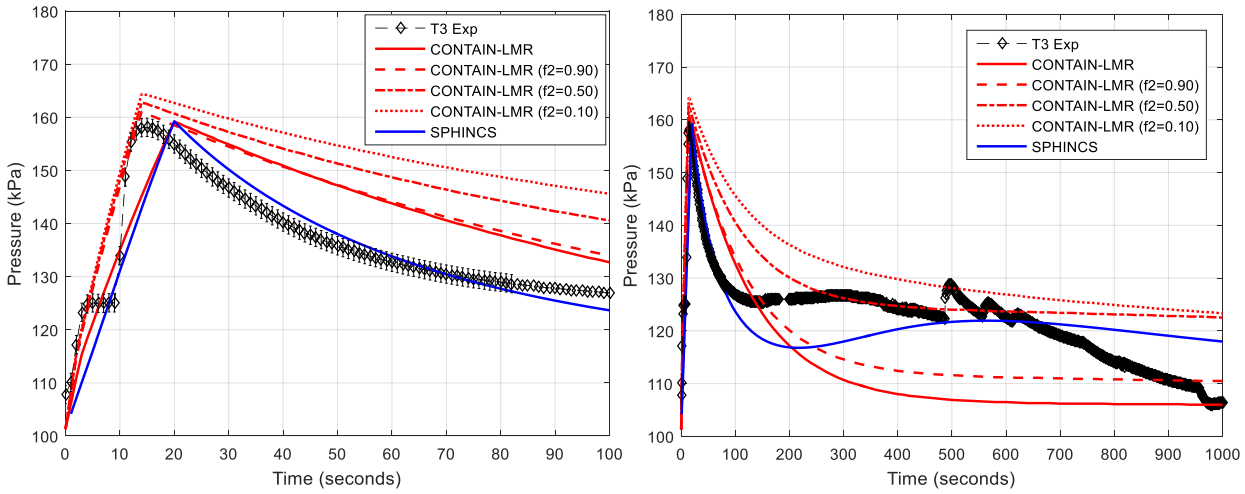

Figure 3-5. T3 pressure responses for pool fire parameter f2 sensitivity analysis for CONTAIN-LMR (red lines) and SPHINCS (blue line). Short term responses are shown on the left and long term responses are shown on the right.

Table 3-5. Total amount of T3 sodium combustion from pool for different pool fire parameter f2 values.

Pool Fire Parameter, *f2*	CONTAIN-LMR	SPHINCS
1.0 (Best Estimate)	1.27 kg	16.15 kg
0.90	1.22 kg	–
0.50	0.45 kg	–
0.10	0.40 kg	–

For all values of *f2*, including the best estimate case, CONTAIN-LMR overpredicts the pressure response immediately following the spray. Based on the sensitivity analysis in Figure 3-5, this overprediction is likely due to the pool fire model itself. The experimental data suggests that there is a period of time after the spray, where the pool heats up before releasing appreciable energy to the system. On the other hand, CONTAIN-LMR's pool fire model starts releasing energy as soon as the pool is formed. As noted previously, the spray most likely forms several small pools so it is difficult to analyze this phenomenon further with respect to the sodium spray experiments.

The long term responses (right plot of Figure 3-5) have significant variation for varying values of pool fire parameter *f2*. For an *f2* value of 0.5, the long term response coincides with the experimental data at about 300 seconds and appears to match the experimental data afterwards. However, there is a significant difference between the experimental data and the *f2=0.5* response from 20 seconds to 300 seconds.

3.2. Summary of SNL T3 Sodium Spray Fire Analysis

CONTAIN-LMR and SPHINCS show good agreement with the SNL T3 sodium spray fire experimental data during the spray. However, the analysis is complicated by non-continuous sodium spray combustion from about three to nine seconds, as described in Appendix A. CONTAIN-LMR and SPHINCS were able to match the experimental peak pressure using mean sodium droplet diameters of 2.45 mm and 2.75 mm, respectively. SPHINCS aligns with the experimental pressure data more closely than CONTAIN-LMR following the spray. SPHINCS

under predicts the overall pressure response, but seems to capture the delayed, appreciable pool combustion and heat up at about 200 seconds into the experiment.

The sensitivity analysis demonstrates the significance of the mean sodium droplet diameter on the overall vessel response. Mean sodium droplet diameter values of 2.0 mm and 3.0 mm produce drastically different peak pressures due to the "D^2" law. The sensitivity analysis also identified the discrepancy between the reported mass flow rate and the observed experimental peak pressure. Based on this analysis, it is believed that the true spray duration was 14 seconds with a mass flow rate of 1.43 kg/s. The importance of the subsequent pool fire that develops from unburned sodium was also identified. Elevated pressure and temperature responses inside the vessel following the spray were not accurately predicted by CONTAIN-LMR or SPHINCS. For CONTAIN-LMR, the long term pressure and temperature responses are most sensitive to the pool fire model parameter, *f2*. When *f2=1.0*, the long term pressure response is significantly under predicted, whereas when *f2=0.1*, the long term pressure response is over predicted. The pool fire model needs to be investigated with respect to pool fire experiments to understand the pool fire parameters completely.

This page is intentionally left blank.

4. SNL T4 SODIUM SPRAY FIRE MODELING RESULTS

Key input parameters for CONTAIN-LMR and SPHINCS are provided in Table 3-1, which represent the initial conditions of the T4 experiment as closely as possible. Similar to modeling of the T3 experiment, the sodium pool fire formed from unburned sodium during the spray has a substantial effect on the long-term pressure and temperature responses. Since the primary focus of this report is on the spray fire modeling, the default parameters for the sodium pool fire model are used for the T4 simulation. Also, the atmospheric chemistry model is activated.

Similar to the approach taken for the T3 analysis, the mean droplet diameter was varied until the results matched the experimental peak pressure. For the T4 analysis, this approach resulted in a mean droplet diameter of 1.4 mm for CONTAIN-LMR and 1.06 mm for SPHINCS.

The user-defined fraction of peroxide formed during spray combustion was set to 1.0, as was done for modeling the T3 spray fire. Additionally, based on the T3 analysis, the spray duration was set to 14 seconds, or a mass flow rate of 1.43 kg/s, for the CONTAIN-LMR T4 simulation.

Table 4-1. Summary of key input parameters for SNL T4 experiment.

Parameter	CONTAIN-LMR	SPHINCS
Vessel free volume	99 m^3	99 m^3
Vessel thickness	0.11 m	0.11 m
Vessel wall emissivity	0.9 [-]	0.9 [-]
Nozzle height	5.3 m	5.3 m
Sodium outlet nozzle velocity	Terminal Velocity	14.45 m/s
Initial sodium temperature	500°C	500°C
Mean droplet diameter (volumetric mean)	1.25 mm	1.00 mm
Sodium pool fire model	Activated	Activated
Atmospheric chemistry model	Activated	Activated
Initial gas temperature	15°C	15°C
Initial gas pressure	101.3 kPa	101.3 kPa
Oxygen concentration (molar fraction)	0.21 [-]	0.21 [-]
Pool fire parameters (*f1*, *f2*, *f3*, *f4*)	0.5, 1.0, 1.0, 0.0	Ring Pool Fire Model [6]

In addition to the input parameters listed in Table 4-1, there is another important feature of the T4 experiment that must be highlighted. At about 11 seconds, one of the instrumentation ports on the Surtsey vessel ruptured leading to a rapid depressurization of the vessel. Investigations of the videography revealed that there is a high-pitched whistle occurring at about six seconds, which suggests that the port started opening up at about six seconds, with full rupture occurring at 11 seconds.

Based on the videography footage, the port failure was modeled as a leak-before-break scenario in CONTAIN-LMR, as shown in Figure 4-1. The leak-before-break scenario assumes that the area doubles every second, starting at six seconds, until reaching full rupture at 11 seconds. The final port diameter is 0.152 m (six inches) which equates to an area of 1.82×10^{-2} m^2. Note that this leak-before-break scenario is only modeled in CONTAIN-LMR by modeling of a flow path from the vessel to the environment.

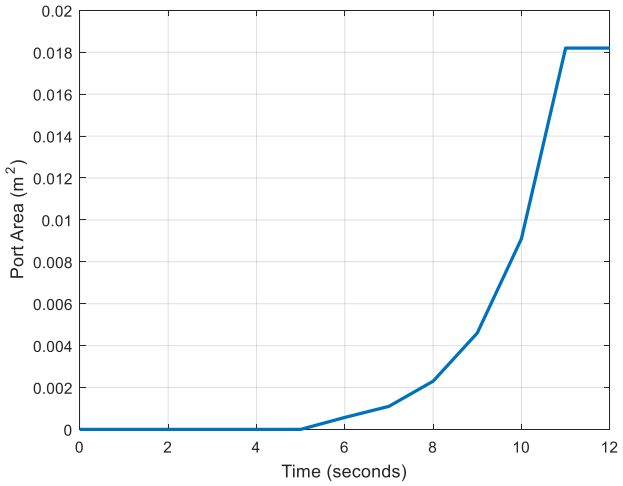

Figure 4-1. Assumed port area for modeling leak-before-break port failure in the T4 experiment.

Since original SPHINCS code has only simplified gas release model, where a flow rate and duration is set as an input data, the following leak model was implemented. When the pressure ratio (ambient pressure/containment pressure) is smaller than a critical value (equal to 0.53 in air), the leak velocity is set to the speed of sound in air.

$$v = \sqrt{\frac{\kappa R T}{M}} \tag{4-1}$$

Here, κ, R, T and M are the specific heat ratio of air (equal to 1.403), the universal gas constant, the gas temperature and the molecular weight of air (equal to 28.966×10^{-3} kg/mol), respectively. For the case of high pressure ratio, a simplified equivalent velocity due to a pressure difference is assumed.

$$v = \sqrt{\frac{2(P_{container} - P_{ambient})}{\rho f}} \tag{4-2}$$

Here, P, ρ and f are the pressure, the gas density and the friction factor, respectively. As concerns the friction factor, a value of 1.5 is assumed considering the contracted and extracted effects. Two cases are considered for SPHINCS predictions of the T4 experiment: port failure area of 1.82×10^{-2} m^2 that does not consider the speed of sound in air and a port failure area of 4.0×10^{-3} m^2 that considers the entire gas release model described by Equations (4-1) and (4-2). It is also noted that SPHINCS models an instantaneous port failure at 11 seconds.

The CONTAIN-LMR and SPHINCS best-estimate results for pressure and temperature responses are shown in Figure 4-2 and Figure 4-3, respectively. The SPHINCS case that does not consider the speed of sound in air is labeled as ‘SPHINCS (wosos)’ and the case that does consider the speed of sound in air is labeled as ‘SPHINCS’ in Figure 4-2 and Figure 4-3. In each figure, short term responses (0-20 seconds) are shown on the left and long term responses (0-100 seconds) are shown on the right. Note that the short term and long term time ranges differ from those defined in the T3 results.

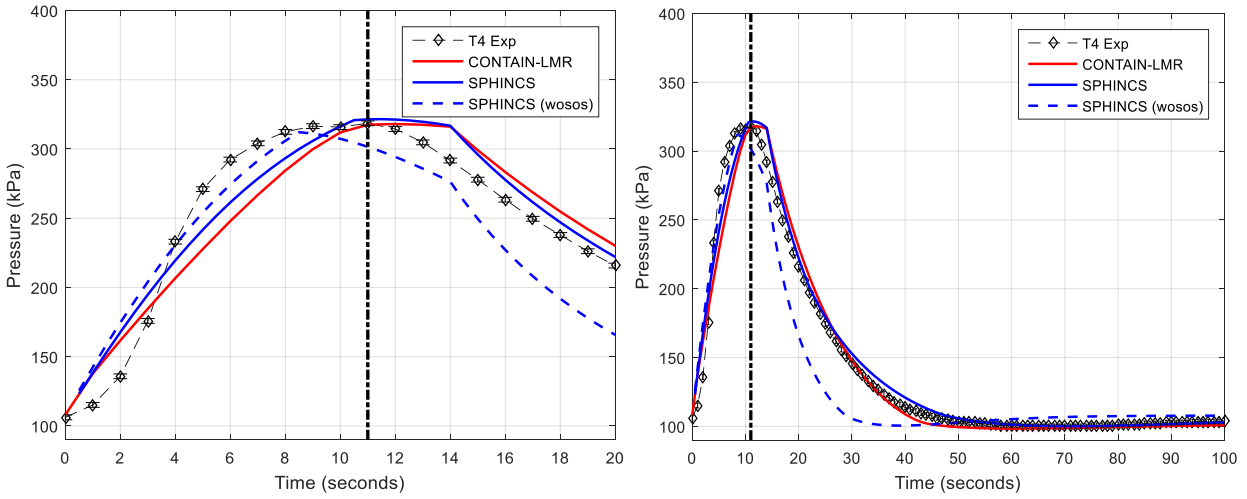

Figure 4-2. T4 pressure responses for best-estimate inputs for CONTAIN-LMR (red line), SPHINCS considering speed of sound in air (blue line), and SPHINCS not considering speed of sound in air (dashed blue line) compared to T4 experimental data. Short term responses are shown on the left and long term responses are shown on the right.

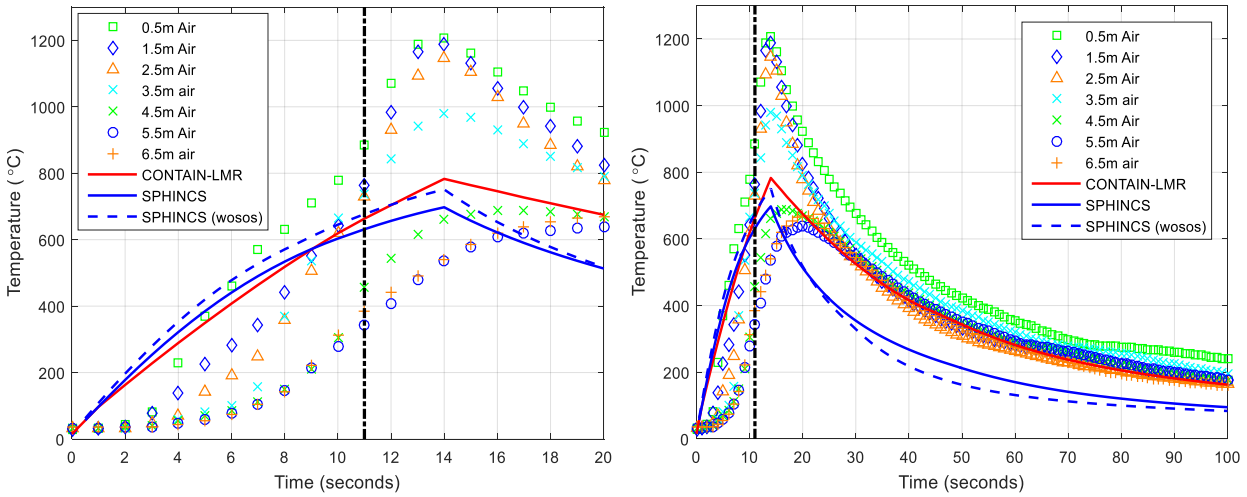

Figure 4-3. T4 temperature responses for best-estimate inputs for CONTAIN-LMR (red line), SPHINCS considering speed of sound in air (blue line), and SPHINCS not considering speed of sound in air (dashed blue line) compared to T4 experimental data. Short term responses are shown on the left and long term responses are shown on the right.

CONTAIN-LMR and SPHINCS show good agreement with the experimental data using the parameters defined in Table 4-1. Both codes over predict the pressure response (Figure 4-2) during the first three seconds, followed by under predicting from 3-11 seconds. From three to six seconds, the experimental data has a large rate of pressure increase which suggests that more energy, which equates to smaller droplet diameter, is being added to the vessel than predicted by either code. The port failure makes this analysis more complicated because by reducing the droplet diameters in either code, the peak pressure would be over predicted. Both codes do not capture the time at which rapid depressurization begins to occur, and instead have an elevated pressure that persists beyond the full port failure. This is either due to inaccurate port failure times or due to the spray fire combustion energy being capable of maintaining an extended elevated pressure response. This will be explored in the sensitivity analysis. Note also that the sets of thermocouple measurements have

large temperature differentials between them that make it difficult to compare them to the vessel temperature results produced by CONTAIN-LMR and SPHINCS; e.g., at 13 seconds, thermocouple 0.5m Air and 6.5m Air have a temperature difference of about 698°C.

CONTAIN-LMR shows excellent agreement with the long term responses (right plots of Figure 4-2 and Figure 4-3) following the port failure and termination of the spray. Similar to the T3 spray discussion, it is likely that multiple pools formed from unburned sodium during the spray. CONTAIN-LMR uses a single pool model for the unburned sodium but this does not seem to impact the long term responses for the T4 experiment.

Table 4-2. Total sodium burned during SNL T4 spray and pool fires for CONTAIN-LMR and SPHINCS.

	CONTAIN-LMR	SPHINCS
Sodium Spray Fire	12.79 kg	17.45 kg
Sodium Pool Fire	0.75 kg	2.54 kg

4.1. SNL T4 Sodium Spray Fire Sensitivity Analysis

The following sections highlight sensitivity of the spray fire models as well as sensitivities addressing experimental uncertainties for the SNL T4 experiment. The sensitivity analysis only compares pressure responses because including the temperature responses would result in numerous lines on a single plot which reduces the ability to interpret the results meaningfully.

4.1.1. Sodium Mean Droplet Diameter Sensitivity

Similar to the T3 spray fire sensitivity analysis, the mean sodium droplet diameter was varied to investigate the overall effect. The CONTAIN-LMR best estimate mean sodium droplet diameter for the T4 experiment is a diameter of 1.25 mm and for SPHINCS it is 1.00 mm, as reported in Table 4-1. The sensitivity analysis for the T4 experiment explored mean droplet diameter values of 1.0 mm and 2.0 mm for CONTAIN-LMR and a value of 2.0 mm for SPHINCS, which is plotted in Figure 4-4.

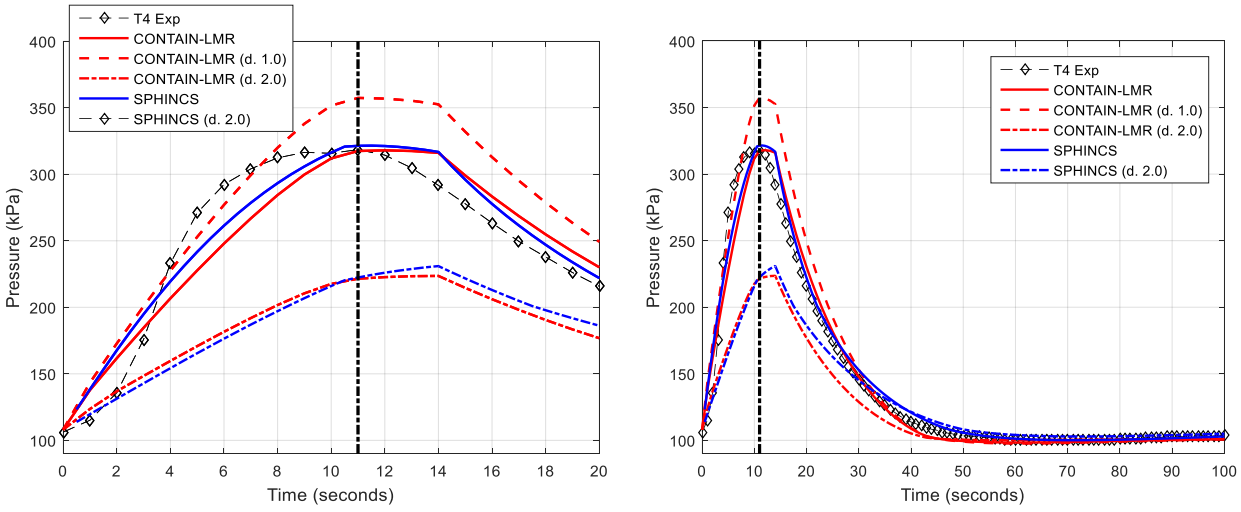

Figure 4-4. T4 pressure responses for mean droplet diameter sensitivity analysis for CONTAIN-LMR (red lines) and SPHINCS (blue lines). Short term responses are shown on the left and long term responses are shown on the right.

Table 4-3. Total amount of sodium combustion during T4 spray for each mean droplet diameter input.

Mean Droplet Diameter	CONTAIN-LMR	SPHINCS
Best Estimate (see Table 4-1)	12.79 kg	17.45 kg
1.0 mm	15.83 kg	17.45 kg
2.0 mm	6.74 kg	7.73 kg

For a mean droplet diameter of 1.0 mm, the peak pressure increase for CONTAIN-LMR was about 13% greater than the best-estimate case (1.25 mm). For a mean droplet diameter of 2.0 mm, both codes resulted in a decrease of the overall peak pressure. The total sodium combusted during the spray for each mean droplet diameter is provided in Table 4-3.

4.1.2. Port Failure Time Sensitivity

It was estimated that the port failure occurred at about 11 seconds. The CONTAIN-LMR and SPHINCS results show a slightly delayed depressurization which suggests that the port failure occurred slightly earlier. Keeping all other parameters equal to values in Table 4-1, port failure time of nine seconds is hypothesized, the results of which are shown in Figure 4-5.

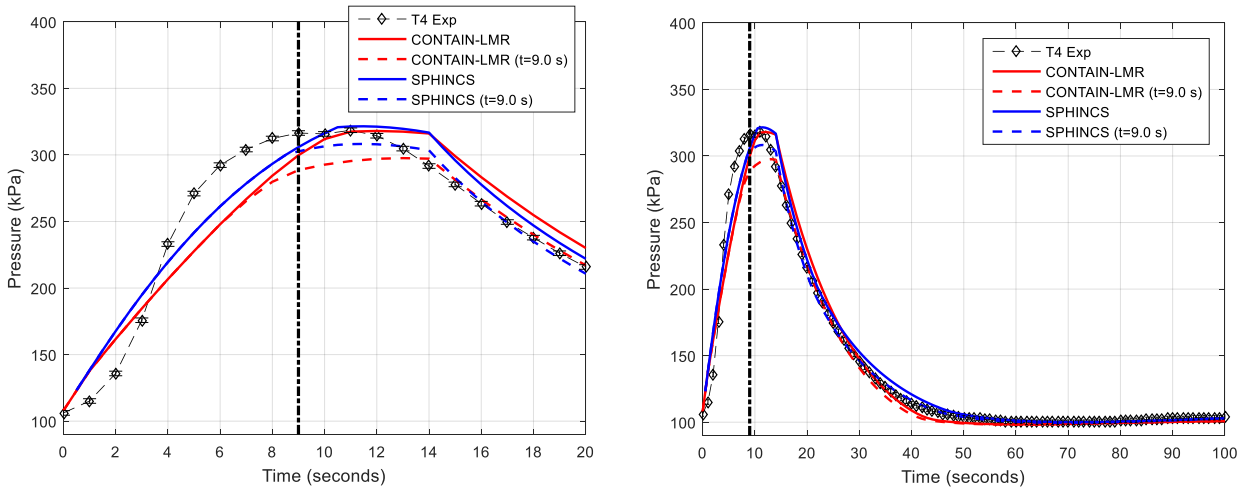

Figure 4-5. T4 pressure responses for port failure time sensitivity analysis for CONTAIN-LMR (red lines) and SPHINCS (blue lines). Short term responses are shown on the left and long term responses are shown on the right.

Adjusting the port failure time to nine seconds results in a lower overall peak pressure for both CONTAIN-LMR and SPHINCS. In the SPHINCS code, port failure occurs instantaneously at nine seconds which differs from the leak-before-break scenario modeled in CONTAIN-LMR. Both codes still predict a slight pressure increase even after reaching full port failure. Thus, the delay observed in the best-estimate cases are more closely correlated with the spray duration than with the port failure opening.

4.2. Summary of SNL T4 Sodium Spray Fire Analysis

The port failure of the SNL T4 experiment make accurate comparisons difficult. The experimental data suggests that there are three phases of vessel response with respect to the spray fire: a short

exponential increase, followed by a short steady-state burn, and finally the response to the port failure causing the pressure to be steady for several seconds while the spray fire persists. Despite the lack of a long, steady spray fire, the two codes show good agreement with the experimental data for both short and long term responses. The sensitivity analysis shows that the sodium spray fire duration of 14 seconds (1.43 kg/s) is responsible for the elevated pressure responses extending beyond the port failure observed for CONTAIN-LMR. SPHINCS depressurization results are mostly impacted by the exiting gas velocity.

5. SUMMARY OF SODIUM SPRAY FIRE RESULTS

CONTAIN-LMR and SPHINCS were compared to two sodium spray fire experiments performed at SNL: SNL T3 experiment and SNL T4 experiment. Both experiments presented difficulties that challenged accurate modeling. The T3 experiment went through a period of non-combustion which is not incorporated into the continuous combustion model. The T4 experiment experienced an unplanned port failure at about 11 seconds into the experiment.

Despite these difficulties, both codes were compared to experiments. The code-to-code comparison showed good agreement with the T3 experiment during the spray fire duration. This experiment also highlighted the importance of the subsequent sodium pool fire that develops from unburned sodium during the spray. The sodium pool fire is not nearly as energetic as the spray fire, but it does provide enough energy to keep the vessel pressure and temperature elevated for an extended period of time. SPHINCS shows better agreement in modeling the sodium pool fire over time due to the more sophisticated ring pool fire model.

The T4 experiment did not have the combustion issues seen in the T3 experiment, but it did experience a port failure that caused the vessel to rapidly depressurize at about 11 seconds. CONTAIN-LMR and SPHINCS show good agreement with the experimental results up to and following the port failure.

The sensitivity analysis showed the pressure response, temperature response, and amount of sodium combusted during the spray is significantly sensitive to the mean droplet diameter. This is to be expected to the "D^2" law that is used in the spray fire models for CONTAIN-LMR and SPHINCS. The sensitivity analysis also resolved several unknown experimental and code characteristics with respect to the SNL T3 and T4 experiments.

Future analysis will look more closely at sodium pool fires. These analyses will provide further understanding of the impact of the sodium pool fire parameters used in CONTAIN-LMR as well as provide further validation of the ring pool fire model used in SPHINCS.

This page is intentionally left blank.

REFERENCES

[1] Itoh, K., et al., *Technical Report on Monju's Sodium Leak Incident*, Journal of Atomic Energy Society Japan, 1997.

[2] Murata, K.K., et al., *User's Manual for CONTAIN 1.1: A Computer Code for Severe Nuclear Reactor Accident Containment Analysis*, NUREG/CR-5026, SAND87-2309, Sandia National Laboratories, Albuquerque, NM, November 1989.

[3] Murata, K.K., et al., *CONTAIN-LMR/1B-Mod. 1, A Computer Code for Containment Analysis of Accidents in Liquid Metal Cooled Reactors*, SAND91-1490, Sandia National Laboratories, Albuquerque, NM, January 1993.

[4] Humphries, L.L., et al., *MELCOR Computer Code Manuals – Vol. 1, Primer and User's Guide, Version 2.1.6840*, SAND2015-6691R, Sandia National Laboratories, Albuquerque, NM, August 2015.

[5] Humphries, L.L. and D.L.Y. Louie, *MELCOR/CONTAIN LMR Implementation Report - FY16 Progress*, SAND2016-12101, Sandia National Laboratories, Albuquerque, NM, November 2016.

[6] Yamaguchi, A. and Y. Tajima, *Validation Study of Computer Code SPHINCS for Sodium Fire Safety Evaluation of Fast Reactor*, Nuclear Engineering and Design, 2003, **219**: p. 19-34.

[7] Olivier, T.J., T.K. Blanchat, V.G. Figueroa, J.C. Hewson and S.P. Nowlen, *Metal Fires and Their Implications for Advance Reactors Part 3: Experimental and Modeling Results*, SAND2010-7113, Sandia National Laboratories, Albuquerque, NM, October 2010.

[8] Tsai, S.S., *The NACOM Code for Analysis of Postulated Sodium Spray Fires in LMFBRs*, NUREG/CR-1405, BNL-NUREG-51180, Brookhaven National Laboratories, Upton, NY, March 1980.

[9] Tsai, S.S., *Surface Oxidation Process Prior to Ignition of a Sodium Droplet*, Trans. Am. Nucl. Soc., 1977, **27**: p. 524.

[10] Ranz, W.E. and W.R. Marshall, *Evaporation from Drops*, Chemical Engineering Progress, 1952, **48**(4): p. 173-180.

[11] Beiriger, P., et al., *SOFIRE II User Report*, Atomics International Division, Rockwell International, Canoga Park, CA, 1973.

[12] Scholtyssek, W. and K.K. Murata, *Sodium Spray and Jet Fire Model Development within the CONTAIN-LMR Code*, SAND93-2200C, Sandia National Laboratories, Albuquerque, NM, 1994.

This page is intentionally left blank.

DISTRIBUTION

1	MS0747	Fred Gelbard	8843
1	MS0748	Matthew Denman	8851
1	MS0748	Andrew J. Clark	8851
1	MS0748	David Louie	8852
1	MS0748	Vincent Mousseau	8852
1	MS0748	Mitch McCrory	8851
2	Japan Atomic Energy Agency Attn: Takashi Takata (1) takata.takashi@jaea.go.jp Attn: Hiroyuki Ohshima ohshima.hiroyuki@jaea.go.jp		
1	MS0899	Technical Library	9536 (electronic copy)

This page is intentionally left blank.


Sandia National Laboratories